How to cite: *Angew. Chem. Int. Ed.* **2021**, *60*, 15313–15316
International Edition: doi.org/10.1002/anie.202104436
German Edition: doi.org/10.1002/ange.202104436

Prebiotic Chemistry

1,1,2-Ethenetriol: The Enol of Glycolic Acid, a High-Energy Prebiotic Molecule

*Artur Mardyukov, Felix Keul, and Peter R. Schreiner**

In memory of Siegfried Hünig

Abstract: *As low-temperature conditions (e.g. in space) prohibit reactions requiring large activation energies, an alternative mechanism for follow-up transformations of highly stable molecules involves the reactions of higher energy isomers that were generated in a different environment. Hence, one working model for the formation of larger organic molecules is their generation from high-lying isomers of otherwise rather stable molecules. As an example, we present here the synthesis as well as IR and UV/Vis spectroscopic identification of the previously elusive 1,1,2-ethenetriol, the higher energy enol tautomer of glycolic acid, a rather stable and hence unreactive biological building block. The title compound was generated in the gas phase by flash vacuum pyrolysis of tartronic acid at 400 °C and was subsequently trapped in argon matrices at 10 K. The spectral assignments are supported by B3LYP/6–311 ++ G(2d,2p) computations. Upon photolysis at λ = 180–254 nm, 1,1,2-ethenetriol rearranges to glycolic acid and ketene.*

High-energy isomers of stable molecules are often the drivers of chemical reactions when no additional source of (external) activation energy is available. This is the case, for example, in the construction of biologically relevant molecules in cold regions of the atmosphere or in extraterrestrial environments.[1–3] There, the energy required for a reaction is often deposited into the structures upon the initial formation of a high-energy isomer or on passing through energy fields; collisions play a minor role because of the very low concentrations even in dense clouds.[4,5] What follows is that the isolation and characterization of high-energy isomers is very helpful in deciphering the formation of complex (organic) molecules that may also be relevant to life. For example, although glycolaldehyde was detected in space in 2000,[6] a mechanism for its gas-phase formation was only put forth in 2018.[7] It involves the higher energy tautomer of formaldehyde, namely hydroxymethylene (H–C̈–OH),[8] reacting with H_2CO in a very facile, low-barrier ($\Delta H^{\ddagger} \approx 1$ kcal mol^{-1}) reaction that can readily occur even at the very low average temperature of space (ca. 2.7 K). Searches in space have failed to find higher mass sugars such as glyceraldehyde and 1,3-dihydroxyacetone.[9] Another molecule of this sort is aminocarbene (H-C̈-NH_2, aminomethylene),[10] the high-energy tautomer of methanimine (CH_2=NH), which is a highly abundant interstellar molecule;[11] it has been proposed to be a precursor for interstellar glycine.[12] The tautomers of acetamide and acetic acid, 1-aminoethenol[13] and 1,1-ethenediol,[14] respectively, whose structures have only very recently been identified, are deemed to be key intermediates in the organic chemistry of space.[15]

Amino acids,[16] polyhydroxylated compounds (polyols)[17] such as sugar alcohols and sugar acids,[18,19] as well as several other organic compounds[20–22] important in biochemistry are thought to have been delivered to prebiotic earth by meteorites and comets,[23] where they may have played a major role in the origin of life. Despite the well-documented detection of these interstellar molecules, the detailed mechanisms of their formation are still elusive for the most part, even though there are some insightful reports on the organic synthesis of more complex molecules in ice experiments that simulate interstellar grains in molecular clouds.[9,24,25]

Glycolic acid (hydroxyacetic acid; **1**), the simplest hydroxycarboxylic acid, is present in many sugar-rich plants and has been found in the Murchison and Bell meteorites,[26–28] along with other polyols (e.g. glycerol) and other hydroxycarboxylic acids (e.g. glyceric acid) that are key precursors to lipids and are relevant to glycolysis.[29] This finding suggests that some fundamentally important biomolecules indeed may have reached earth by meteoritic impacts and that aqueous conditions are not necessarily required for their production. The mechanism for the formation of **1** remains unknown, even though there are some synthetic approaches from simple molecules in simulated ice experiments. In these simulations, irradiation of $H_2O/CH_3OH/NH_3$ and H_2O/CH_3OH ices with ultraviolet light give mixtures of polyols and hydroxycarboxylic acids through free-radical pathways.[30]

In general, enols are important reactive intermediates in organic synthesis[31–33] as well as in biologically relevant reactions.[34] The first interstellar detection of the simplest enol (vinyl alcohol, CH_2=CHOH) in its *syn* and *anti* forms was reported in 2001 from microwave emissions from Sagittarius B2.[35] High-energy phosphoenol pyruvate is found in living organisms and derives from abiotic precursors such as

[*] Dr. A. Mardyukov, F. Keul, Prof. Dr. P. R. Schreiner
Institute of Organic Chemistry, Justus Liebig University
Heinrich-Buff-Ring 17, 35392 Giessen (Germany)
E-mail: prs@uni-giessen.de

Supporting information and the ORCID identification numbers for some of the authors of this article can be found under: https://doi.org/10.1002/anie.202104436.

glycolaldehyde and glyceraldehyde.[36] Several enols have been implicated as the building blocks for the synthesis of carbohydrates in prebiotic cycles.[37,38] For example, 1,2-ethenediol, the enol of glycolaldehyde, has been implied to contribute in the synthesis of prebiotic three-, four-, and five-carbon sugars.[37,38] Herein, we present the preparation as well as the IR and UV/Vis spectroscopic identification of hitherto uncharacterized 1,1,2-ethenetriol (**2**), the high-energy enol tautomer of glycolic acid (**1**). Triol **2** has been implied in mass-spectrometric studies on the ionization products of ethyl glycolate through neutralization and re-ionization;[39] there is no spectroscopic signature available for **2**. The spectroscopic proof for the existence of **2** is important in the context of the abiotic formation of sugar acids. For example, the formation of putative **2** from **1** can be promoted by minerals (e.g. borates),[37,38] where the cycle begins with the aldol reaction of **2** (as the nucleophile) with formaldehyde (as the electrophile) to form glyceric acid. Various phosphate derivatives of glyceric acid including mono- and diphosphoglyceric acids are key biochemical intermediates in glycolysis.

Very recently, we reported the preparation of previously elusive 1,1-ethenediol[14] and 1-aminoethenol,[13] the enols of acetic acid and acetamide, respectively, through flash vacuum pyrolysis (FVP) of the corresponding acids and subsequent product trapping in argon matrices. Turecek et al.[40,41] described the synthesis of several simple neutral enols by the retro-Diels–Alder decomposition of norbornene precursors, and characterized the products by high-resolution mass spectrometry and measurements of the ionization energy in the gas phase. Our strategy for the preparation of **2** is FVP of tartronic acid (**3**) through the reaction **3**→**2** + CO_2 (Scheme 1). After various attempts, we found that 400 °C was the optimal pyrolysis temperature. Pyrolysis of **3** and subsequent trapping of the pyrolysis products at 10 K led to large amounts of CO_2 in the corresponding matrix isolation spectra, indicating almost complete consumption of **3** and confirming the dissociation pathway (Figure S1).

The infrared spectrum of the FVP products of **3** shows several new absorptions, in addition to IR bands of **1** formally derived from **2** by a 1,3[H] migration and the typical impurities (for example, H_2O) often found in FVP matrix-isolation experiments (Figure S1). Structure **1** was identified by comparison with matrix-isolated data of an authentic sample (see below). We also observed new unreported signals that we assign to **2**. Notably, a medium-intensity band at 1761 cm^{-1} is attributed to the C=C stretching mode of **2** (Figure 1), which agrees well with previous IR measurements of other enols (e.g. 1667 cm^{-1}: ethenol;[42] 1712 cm^{-1}: 1,1-ethenediol;[14] 1680 cm^{-1}: 1-aminoethenol).[13] The very prominent bands at 3624, 3619, and 3557 cm^{-1} can be assigned to the OH stretching modes of **2** (Figure S2). The strong band at 1087 cm^{-1} for **2** corresponds to the most characteristic C-O stretching vibration. Intense C-O stretching and C–H out of plane deformation modes were found at 918 and 690 cm^{-1}, respectively, along with bands at 479 and 445 cm^{-1} for the O-H wagging and OCO deformation modes, respectively (Table S1).

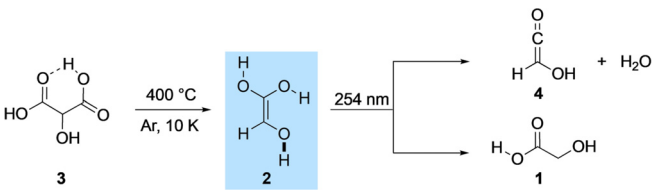

Scheme 1. 1,1,2-Ethenetriol (**2**) generated from tartronic acid (**3**) through pyrolysis and trapping in an argon matrix as well as the subsequent photorearrangement to glycolic acid (**1**) and ketene (**4**).

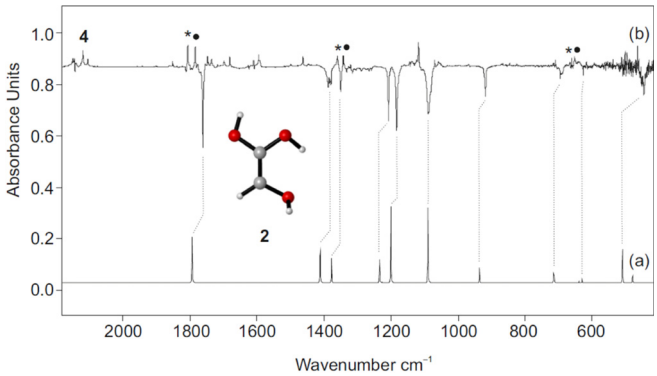

Figure 1. a) IR spectrum of **2** computed at B3LYP/6–311++G(2d,2p) (unscaled). b) IR spectrum showing the pyrolysis product of **3** with subsequent trapping in an argon matrix at 10 K. The IR difference spectrum illustrates the photochemistry of **2** after irradiation with light of $\lambda = 180$–254 nm in argon at 10 K. Downward bands assigned to **2** disappear while upward bands assigned to **1** and **4** (Scheme 1) appear after 15 min irradiation time. Bands labeled with "*" and "●" correspond to the different conformers of **1** ("*": **1aat**; "●": **1gac**).

The assignments of these bands were also verified with a d_4-labeled derivative, since deuteration resulted in characteristic isotopic shifts. For example, the prominent IR band at 1761 cm^{-1} is red-shifted by 34 cm^{-1} (calcd, unscaled: −40 cm^{-1}) in d_4-**2**. As expected, the O-H stretching modes at 3624, 3619, and 2557 cm^{-1} show large red-shifts of 937, 947, and 932 cm^{-1}, respectively (calcd: −1040, 1031, and −1027 cm^{-1}) in d_4-**2**. The C–H stretching and deformation modes at 3122 and 1383 cm^{-1} display red-shifts of 784 and 44 cm^{-1}, respectively (calcd: −837 and −60 cm^{-1}). The O-H deformation modes at 1350 and 1208 cm^{-1} show red-shifts of 171 and 195 cm^{-1}, respectively (calcd: −184 and −213 cm^{-1}). The nice match between the computed (B3LYP/6–311++G(2d,2p)) and experimentally observed frequencies and frequency shifts of **2** and d_4-**2** underscores the successful preparation of these reactive species (Figure 1, Figures S1–S3, Table S1).

The UV/Vis spectrum of matrix-isolated **2** displays a strong transition at $\lambda = 190$ nm, which correlates well with the computed value of $\lambda = 193$ nm ($f = 0.095$) employing TD-B3LYP/6–311++G(2d,2p). This absorption band arises from a HOMO–LUMO + 4 excitation, which corresponds to a π-π* transition (Figure 2).

We also explored the photochemistry of **2**. The challenge here lies in the rich unimolecular photochemistry of **1** present in the matrix, namely conformational isomerizations resulting from irradiation of matrix-isolated **1** with broad-band near-IR/mid-IR light, which has been studied previously.[43,44] We envisaged that irradiation at an appropriate wavelength would allow us to excite **2** selectively. Considering the intense

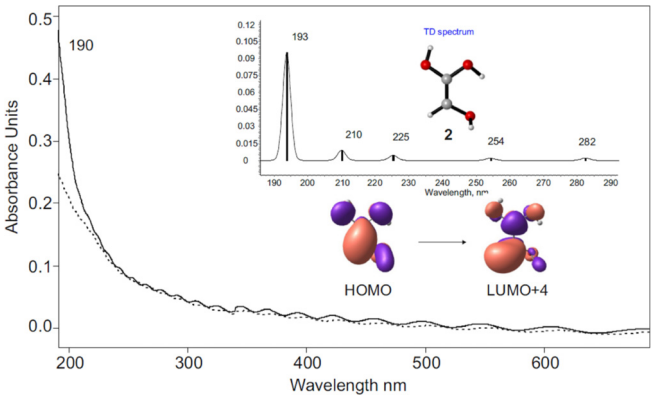

Figure 2. Solid line: UV/Vis spectrum showing the pyrolysis product of **3** with subsequent trapping in an argon matrix at 10 K. Dashed line: after irradiation at $\lambda = 180$–254 nm for 10 min in argon at 10 K. Inset: computed [TD-B3LYP/6–311++G(2d,2p)] electronic transitions of **2**.

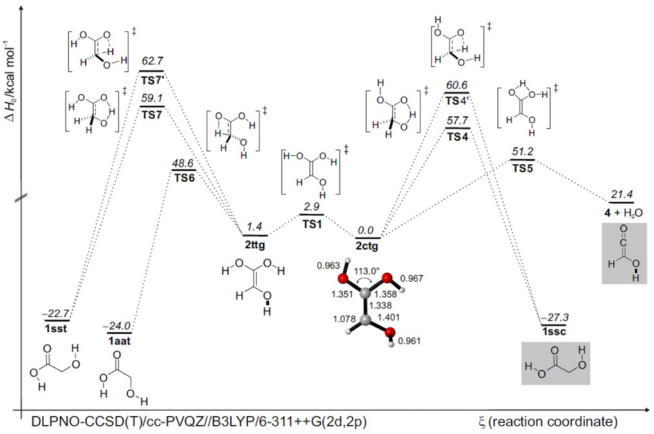

Figure 3. Potential energy hypersurface profile (ΔH_0) in kcal mol^{-1} of the reactions of enol **2** at DLPNO-CCSD(T)/cc-pVQZ//B3LYP/6–311++G(2d,2p) + ZPVE at 0 K. The title compound **2ctg** and the structures in gray boxes have been observed in the present study.

absorption at $\lambda = 190$ nm for matrix-isolated **2**, we irradiated the matrices of the pyrolysis products at $\lambda = 180$–254 nm, which selectively bleached the IR bands of **2** and simultaneously led to the appearance of new IR bands that can readily be matched with **1** (Figure S4). Along with IR bands of **1**, we also observed a strong IR band at 2119 cm^{-1} with an isotopic shift of 5 cm^{-1} (calcd: 7 cm^{-1}) corresponding to the C=O stretching mode of hydroxyketene (**4**), the dehydration product of **2**. It has been shown that irradiation of the most stable conformer of **1** in low-temperature matrices produces higher energy conformers of **1**;[43,44] these results could readily be reproduced here. Note that irradiation of **1ssc** with light of $\lambda = 180$–254 nm leads to the formation of **1aat** and **1gac** (Figure S4). Hence, we did not observe the IR bands of **1ssc** upon irradiation of matrices containing **2ctg** (see below). In accordance with the IR experiments, irradiation of the matrix containing **2** with light of $\lambda = 180$–254 nm led to the disappearance of the UV band at 190 nm.

To support our experimental assignments further, we undertook a detailed computational analysis of the most important intramolecular rearrangements of **2** at DLPNO-CCSD(T)/cc-pVQZ//B3LYP/6–311++G(2d,2p) (including zero-point vibrational energy, ZPVE, denoted as ΔH_0; Figure 3). According to the computations, **2** displays four conformers with *s-cis*, *s-trans*, and *s-gauche* orientations of the OH groups relative to the opposing C–O bond: *s-cis*, *s-trans*, *s-gauche* (**2ctg**); *s-trans*, *s-trans*, *s-gauche* (**2ttg**); *s-cis*, *s-cis*, *s-cis* (**2ccc**); *s-gauche*, *s-gauche*, *s-cis* (**2ggc**). The **2ctg** conformer is predicted to be the most stable conformer with a nonplanar C_1 structure; conformers **2ttg** and **2ccc** are 1.4 and 1.6 kcal mol^{-1} less stable. The activation enthalpies for the **2ctg**→**2ttg** and **2ctg**→**2ccc** conformational isomerizations are 2.9 and 4.4 kcal mol^{-1} (**TS1** and **TS2**; Figure S5), respectively. The **2ggc** conformer is the least stable conformer, with a relative energy of 2.5 kcal mol^{-1}. The activation barrier for the **2ccc**→**2ggc** conformational isomerization is 1.3 kcal mol^{-1}. The experimentally observed IR spectrum of the pyrolysis products nicely matches the computed spectrum of **2ctg**, and only this conformer is present in the matrix (Tables S1 and S2).

The tautomerization of **2ctg** to **1ssc** (note that **1ssc** is the most stable conformer of glycolic acid)[43] proceeds by a double hydrogen-shift mechanism, with a barrier of 57.7 kcal mol^{-1} (**TS4**), involving hydrogen atom transfers from the tetrahedral carbon atom to the hydroxy group, and from the hydroxy group to the oxygen atom (Figure 3). The **2ctg**→**1ssc** interconversion through a conventional [1,3]H-shift mechanism is characterized by an even higher barrier (**TS4′**) of 60.6 kcal mol^{-1}, which is similar to the [1,3]H-shift of 1,1-ethenediol (**6**) to form acetic acid.[14] The fact that we observed characteristic peaks for **1ssc** directly after FVP suggests that the energy is sufficient in the pyrolysis zone for **2ctg** to isomerize to **1ssc** (possibly through a surface-catalyzed reaction). The formation of hitherto unreported free ketene **4**[45] and water from **2ctg** is associated with a barrier of 51.2 kcal mol^{-1}, and so it is unsurprising that **4** can readily be observed under our reaction conditions. In analogy to **2ctg**, the related H-shifts from **2ttg** to **1sst** are characterized by high barriers of 59.1 and 62.7 kcal mol^{-1} (**TS7** and **TS7′**). The [1,3]H-shift from **2ttg** to **1aat** is accompanied by an activation barrier (**TS6**) of 48.6 kcal mol^{-1}. The activation barriers (**TS10** and **TS11**) for the **1ssc**→**1gas** and **1gac**→**1aat** interconversions are 5.1 and 14 kcal mol^{-1} (Figure S7), respectively.

For a better estimate of the stability and expected reactivity of **2**, we compared the HOMO–LUMO energy differences of **2** with other enols (Figure S8). The addition of one OH group increases the HOMO energy, thereby resulting in a smaller HOMO–LUMO gap in **2** (−0.196 eV) compared to 1,1-ethenediol (**6**; −0.207 eV) and ethenol (−0.235 eV). This implies that **2** should be the best nucleophile in this series. The hydroxy group, as a strong π-donor, increases the electron density of the C=C bond, which is also evident from the experimentally observed C=C stretching vibration of **2** that is blue-shifted by 49 cm^{-1} in comparison to the C=C stretching vibration at 1712 cm^{-1} for 1,1-ethendiol.[14] As expected, **2** does not exhibit quantum mechanical hydrogen tunneling to **1** because the barriers are too high and too wide.[46,47] We did not observe a decrease in the IR bands of **2** at 10 K even after five days in the dark.

In summary, we present the first IR as well as UV/vis spectroscopic characterization of 1,1,2-ethenetriol, the higher energy isomer of prebiotically important glycolic acid. The spectroscopic proof for the existence of 1,1,2-ethenetriol is important in the context of the abiotic formation of sugar acids, for which enols are likely to be important intermediates. Our study will help identify the title compound in extra-terrestrial environments.

Acknowledgements

This work was supported by the Volkswagen Foundation ("What is Life" grant 92 748). Open access funding enabled and organized by Projekt DEAL.

Conflict of interest

The authors declare no conflict of interest.

Keywords: enols · glycolic acid · photochemistry · prebiotic chemistry

[1] J. L. Bada, *Chem. Soc. Rev.* **2013**, *42*, 2186 – 2196.
[2] S. L. Miller, H. C. Urey, *Science* **1959**, *130*, 245 – 251.
[3] K. Ruiz-Mirazo, C. Briones, A. de la Escosura, *Chem. Rev.* **2014**, *114*, 285 – 366.
[4] R. T. Garrod, S. L. Widicus Weaver, E. Herbst, *Astrophys. J.* **2008**, *682*, 283 – 302.
[5] A. Nummelin, P. Bergman, A. Hjalmarson, P. Friberg, W. M. Irvine, T. J. Millar, M. Ohishi, S. Saito, *Astrophys. J. Suppl. Ser.* **2000**, *128*, 213 – 243.
[6] J. M. Hollis, F. J. Lovas, P. R. Jewell, *Astrophys. J.* **2000**, *540*, L107.
[7] A. K. Eckhardt, M. M. Linden, R. C. Wende, B. Bernhardt, P. R. Schreiner, *Nat. Chem.* **2018**, *10*, 1141 – 1147.
[8] P. R. Schreiner, H. P. Reisenauer, F. C. Pickard, A. C. Simmonett, W. D. Allen, E. Matyus, A. G. Csaszar, *Nature* **2008**, *453*, 906 – 909.
[9] C. R. Arumainayagam, R. T. Garrod, M. C. Boyer, A. K. Hay, S. T. Bao, J. S. Campbell, J. Wang, C. M. Nowak, M. R. Arumainayagam, P. J. Hodge, *Chem. Soc. Rev.* **2019**, *48*, 2293 – 2314.
[10] A. K. Eckhardt, P. R. Schreiner, *Angew. Chem. Int. Ed.* **2018**, *57*, 5248 – 5252; *Angew. Chem.* **2018**, *130*, 5346 – 5350.
[11] P. D. Godfrey, R. D. Brown, B. J. Robinson, M. W. Sinclair, *Astrophys. Lett.* **1973**, *13*, 119 – 121.
[12] T. Suzuki, M. Ohishi, T. Hirota, M. Saito, L. Majumdar, V. Wakelam, *Astrophys. J.* **2016**, *825*, 79/71 – 79/14.
[13] A. Mardyukov, F. Keul, P. R. Schreiner, *Chem. Sci.* **2020**, *11*, 12358 – 12363.
[14] A. Mardyukov, A. K. Eckhardt, P. R. Schreiner, *Angew. Chem. Int. Ed.* **2020**, *59*, 5577 – 5580; *Angew. Chem.* **2020**, *132*, 5625 – 5628.
[15] L. Foo, A. Surányi, A. Guljas, M. Szőri, J. J. Villar, B. Viskolcz, I. G. Csizmadia, A. Rágyanszki, B. Fiser, *Mol. Astrophys.* **2018**, *13*, 1 – 5.
[16] K. Kvenvolden, J. Lawless, K. Pering, E. Peterson, J. Flores, C. Ponnamperuma, I. R. Kaplan, C. Moore, *Nature* **1970**, *228*, 923 – 926.
[17] Y. Furukawa, Y. Chikaraishi, N. Ohkouchi, N. O. Ogawa, D. P. Glavin, J. P. Dworkin, C. Abe, T. Nakamura, *Proc. Natl. Acad. Sci. USA* **2019**, *116*, 24440 – 24445.
[18] M. P. Bernstein, J. P. Dworkin, S. A. Sandford, G. W. Cooper, L. J. Allamandola, *Nature* **2002**, *416*, 401 – 403.
[19] G. Cooper, A. C. Rios, *Proc. Natl. Acad. Sci. USA* **2016**, *113*, E3322 – E3331.
[20] M. P. Callahan, K. E. Smith, H. J. Cleaves II, J. Ruzicka, J. C. Stern, D. P. Glavin, C. H. House, J. R. Dworkin, *Proc. Natl. Acad. Sci. USA* **2011**, *108*, 13995 – 13998.
[21] P. G. Stoks, A. W. Schwartz, *Nature* **1979**, *282*, 709 – 710.
[22] A. Shimoyama, R. Ogasawara, *Origins Life Evol. Biospheres* **2002**, *32*, 165 – 179.
[23] F. Goesmann, H. Rosenbauer, J. H. Bredehoeft, M. Cabane, P. Ehrenfreund, T. Gautier, C. Giri, H. Krueger, L. Le Roy, A. J. MacDermott, S. McKenna-Lawlor, U. J. Meierhenrich, G. M. M. Caro, F. Raulin, R. Roll, A. Steele, H. Steininger, R. Sternberg, C. Szopa, W. Thiemann, S. Ulamec, *Science* **2015**, *349*, aab0689-1 – 3.
[24] C. Meinert, I. Myrgorodska, P. de Marcellus, T. Buhse, L. Nahon, S. V. Hoffmann, L. Le Sergeant d'Hendecourt, U. J. Meierhenrich, *Science* **2016**, *352*, 208 – 212.
[25] P. de Marcellus, C. Meinert, I. Myrgorodska, L. Nahon, T. Buhse, L. Le Sergeant d'Hendecourt, U. J. Meierhenrich, *Proc. Natl. Acad. Sci. USA* **2015**, *112*, 965 – 970.
[26] G. Cooper, N. Kimmich, W. Belisle, J. Sarlnana, K. Brabham, L. Garrel, *Nature* **2001**, *414*, 879 – 883.
[27] Y. Kebukawa, A. L. D. Kilcoyne, G. D. Cody, *Astrophys. J.* **2013**, *771*, 19.
[28] A. A. Monroe, S. Pizzarello, *Geochim. Cosmochim. Acta* **2011**, *75*, 7585 – 7595.
[29] K. B. Muchowska, S. J. Varma, J. Moran, *Nature* **2019**, *569*, 104 – 107.
[30] C. Zhu, A. M. Turner, C. Meinert, R. I. Kaiser, *Astrophys. J.* **2020**, *889*, 134.
[31] K. Schank, *Synthesis* **1972**, 176 – 190.
[32] U. Hertenstein, S. Huenig, H. Reichelt, R. Schaller, *Chem. Ber.* **1986**, *119*, 699 – 721.
[33] E. Hirsch, S. Huenig, H. U. Reissig, *Chem. Ber.* **1982**, *115*, 3687 – 3696.
[34] K. Miyamoto, H. Ohta in *Future Directions in Biocatalysis* (Ed.: T. Matsuda), Elsevier Science B.V., Amsterdam, **2007**, pp. 305 – 343.
[35] B. E. Turner, A. J. Apponi, *Astrophys. J.* **2001**, *561*, L207 – L210.
[36] A. J. Coggins, M. W. Powner, *Nat. Chem.* **2017**, *9*, 310 – 317.
[37] A. Ricardo, M. A. Carrigan, A. N. Olcott, S. A. Benner, *Science* **2004**, *303*, 196.
[38] H.-J. Kim, A. Ricardo, H. I. Illangkoon, M. J. Kim, M. A. Carrigan, F. Frye, S. A. Benner, *J. Am. Chem. Soc.* **2011**, *133*, 9457 – 9468.
[39] D. Suh, J. T. Francis, J. K. Terlouw, P. C. Burgers, R. D. Bowen, *Eur. Mass Spectrom.* **1995**, *1*, 545 – 559.
[40] F. Tureček, *Tetrahedron Lett.* **1984**, *25*, 5133 – 5134.
[41] F. Tureček, L. Brabec, J. Korvola, *J. Am. Chem. Soc.* **1988**, *110*, 7984 – 7990.
[42] M. Hawkins, L. Andrews, *J. Am. Chem. Soc.* **1983**, *105*, 2523.
[43] A. Halasa, L. Lapinski, I. Reva, H. Rostkowska, R. Fausto, M. J. Nowak, *J. Phys. Chem. A* **2014**, *118*, 5626 – 5635.
[44] C. M. Nunes, I. Reva, R. Fausto, *Phys. Chem. Chem. Phys.* **2019**, *21*, 24993 – 25001.
[45] Z. Mielke, M. Mucha, A. Bil, B. Golec, S. Coussan, P. Roubin, *ChemPhysChem* **2008**, *9*, 1774 – 1780.
[46] P. R. Schreiner, *J. Am. Chem. Soc.* **2017**, *139*, 15276 – 15283.
[47] A. Fernández-Ramos, *Angew. Chem. Int. Ed.* **2013**, *52*, 8204 – 8205; *Angew. Chem.* **2013**, *125*, 8362 – 8363.

Manuscript received: March 30, 2021
Revised manuscript received: April 19, 2021
Accepted manuscript online: May 5, 2021
Version of record online: June 4, 2021

